# (2 + 1)-Dimensional Directed Polymer in a Random Medium: Scaling Phenomena and Universal Distributions

Timothy Halpin-Healy
*Physics Department, Barnard College, Columbia University, New York, New York 10027, USA*
(Received 27 June 2012; published 23 October 2012)

We examine numerically the zero-temperature (2 + 1)-dimensional directed polymer in a random medium, along with several of its brethren via the Kardar-Parisi-Zhang (KPZ) equation. Using finite-size and KPZ scaling *Ansätze*, we extract the universal distributions controlling fluctuation phenomena in this canonical model of nonequilibrium statistical mechanics. Specifically, we study point-point, point-line, and point-plane directed polymer geometries, scenarios which yield higher-dimensional analogs of the Tracy-Widom distributions of random matrix theory. Our analysis represents a robust, multifaceted numerical characterization of the 2 + 1 KPZ universality class and its limit distributions.

DOI: 10.1103/PhysRevLett.109.170602 PACS numbers: 05.10.Gg, 05.40.−a, 64.70.qj

For the past 25 years, the celebrated work [1] of Kardar, Parisi, and Zhang (KPZ) has held center-stage within the realm of nonequilibrium statistical mechanics. Invoking the spirit of Landau, these authors put forth a continuum description of kinetically roughened microscopic models of stochastic growth, capturing their essential universal scaling behaviors. In this context, KPZ consider a fluctuating height variable $h(\mathbf{x}, t)$, evolving as:

$$\partial_t h = \nu \nabla^2 h + \frac{1}{2}\lambda(\nabla h)^2 + \sqrt{D}\eta(\mathbf{x}, t),$$

where $\mathbf{x}$ is a $d$-dimensional vector in the substrate plane of growth, $\nu$, $\lambda$, and $D$ are phenomenological parameters, the last setting the strength of the stochastic noise, which is uncorrelated in space and time and possessing variance $\langle \eta_{\mathbf{x}',t'}\eta_{\mathbf{x},t}\rangle = \delta^d(\mathbf{x}' - \mathbf{x})\delta(t' - t)$. As a diffusive Langevin equation supplemented by rotationally invariant nonlinearity, the KPZ equation has become a fundamental equation of 21st-century theoretical physics. The simple Hopf-Cole transformation, $h(\mathbf{x}, t) = (2\nu/\lambda)\ln Z(\mathbf{x}, t)$, maps KPZ stochastic growth onto the equilibrium statistical physics of directed polymers in a random medium (DPRM); i.e., a Schrödinger equation with multiplicative disorder for the restricted partition function $Z(\mathbf{x}, t)$:

$$\partial_t Z = \nu \nabla^2 Z + (\lambda\sqrt{D}/2\nu)Z\eta,$$

itself a paradigmatic model of ill-condensed matter physics. By contrast, the substitution $v = \nabla h$ takes one to the well-studied noisy Burgers equation, which in 1 + 1 dimensions, ties the KPZ growth and DPRM problems to the rather fertile and amply harvested field of driven lattice gases (DLG), beloved by the mathematics community. Consequently, investment in the KPZ triumvirate of stochastic growth, directed polymers, and driven lattice gases, pays off handsomely. Early analytical, numerical and experimental work on the KPZ class of problems, well documented in reviews [2], focussed on scaling exponents, universal amplitude ratios [3], and a tantalizing glimpse [4] of full probability distributions (PDFs) of the 1 + 1 KPZ class. The last twelve years have witnessed several spectacular advances within the context of the 1 + 1 KPZ equation, a consequence of mathematicians bringing a vast arsenal of analytical tools to bear on the matter [5]. First, Johansson [6] revealed that the height fluctuations of the 1 + 1 single-step model [7] grown from a point seed were captured by the Tracy-Widom (TW) distribution [8] of the Gaussian unitary ensemble (GUE), an astounding, entirely unanticipated discovery that immediately connected the 1 + 1 KPZ triumvirate to a huge and distinguished university class of Gaussian random matrices. Shortly thereafter, Prähofer and Spohn [9] observed that 1 + 1 polynuclear growth mapped directly onto the Ulam problem regarding statistics of the longest increasing subsequence of random permutations, also governed [10] by TW GUE. These authors made it quite clear, as well, that a different TW distribution, one tied to the Gaussian orthogonal ensemble (GOE), was relevant to 1 + 1 KPZ stochastic growth from a flat substrate initial condition (IC). A decade later, tour de force exact solutions of the 1 + 1 KPZ-DPRM problem, including the full time evolution of the universal PDFs to their asymptotic TW forms was managed by independent researchers using complementary DLG [11] and replica-theoretic DPRM approaches [12]. Simultaneously, in a series of beautiful experiments, Takeuchi and Sano [13] managed to observe both TW GOE and GUE statistics in a 1 + 1 KPZ kinetic roughening experiment down to probabilities as small as $10^{-4}$. The crucial role of KPZ scaling theory in deciphering these experiments, as well as providing a deeper understanding of the 1 + 1 exact solutions, has been much emphasized recently by Spohn [14].

Our purpose here is to unearth the rich universality of the 2 + 1 KPZ class, a problem for which there are no known exact results and where, furthermore, the higher dimensionality allows additional geometric possibilities. We focus attention on 7 distinct models within this class: (a) 4 DPRM variations, (b) RSOS—the classic "restricted solid-on-solid" model of KPZ kinetic roughening,

 

(c) a direct Eulerian integration of the $2+1$ KPZ equation and, finally, (d) 2D driven dimers—an octahedral KPZ deposition model due to Kelling and Ódor [15], which permits a direct interpretation in terms of a 2D DLG of dimers in the plane. Within the DPRM sector of the $2+1$ KPZ class, we have restricted ourselves to $T=0$, so our DPRM simulations amount to a transfer matrix calculation of the *globally optimal directed walk through a 3D lattice of random energy sites,* the total path energy being the sum of the site energies visited along the way. The three relevant $2+1$ DPRM geometries are the point-point, point-line, and point-plane. In all instances, the directed walk commences at the origin, but in the point-point geometry the endpoint is also fixed, while the others constrain said endpoint to line or plane, respectively. Regarding the PDF from which the individual site energies are drawn, we stick to the main KPZ story line, considering disorder that is spatiotemporally uncorrelated, but pulled from uniform (u), Gaussian (g), or exponential (e) distributions. There is freedom, too, in specifying the crystallographic nature of the 3D lattice (sc, fcc, or bcc), as well as the possible inclusion of a microscopic elastic energy cost, typically denoted $\gamma$ [3], associated with transverse steps. Among our DP models, we consider: (i) $e3_{\mathrm{fcc}}$ DPRM, in which trajectories emanate from the origin (0,0,0), proceed into the first octant, travel on average along the (1,1,1) direction, collecting random site energies $\varepsilon$ drawn from the exponential distribution $p(\varepsilon)=e^{-|\varepsilon|}$. Our $e3_{\mathrm{fcc}}$ model generalizes to a higher dimension the $1+1$ DPRM in the wedge geometry [16] which, with exponentially distributed site energies, is a strict counterpart to the $1+1$ single-step KPZ growth model and totally asymmetric DLG, solved rigorously by Johannson [6], who made explicit the extraordinary connection of $1+1$ KPZ to TW GUE random matrix statistics. For this reason alone, the $e3_{\mathrm{fcc}}$ DPRM plays a special role in our analysis, and is examined in all three geometries. We mention, too, that this particular model is the precise $2+1$ DPRM analog of the 3D corner growth model examined by Olejarz *et al.* [17] whose focus was on the unknown macroscopic limit shape, rather than the height fluctuations which concern us here. Our own investigation of the *anisotropic line tension* of the $2+1$ $e3_{\mathrm{fcc}}$ DPRM, relevant to the limit shape geometry of the corner growth model, will be discussed elsewhere. Other DP models include (ii) $g4_{\mathrm{bcc}}$: body-centered cubic arrangement, with Gaussian distributed site energies (zero mean, unit variance), (iii) $u5_{\mathrm{sc}}$: simple cubic lattice, site energies drawn uniformly from $(0,1)$, with elastic energy cost $\gamma=1$, and finally, (iv) $g5_{\mathrm{sc}}$: simple cubic again, same $\gamma$, but with Gaussian energies, this time zero mean, variance $\frac{1}{4}$. In the last instances, the transfer matrix code is built upon an update rule of the form: $E_{x',t+1}=\varepsilon+\mathrm{Min}[E_{x_1,t},E'_{x_2,t},E'_{x_3,t},E'_{x_4,t},E'_{x_5,t}]$, where $x_n$ locates the $n$th nearest neighbor in the preceding plane (i.e., time slice), $E'_{x_n,t}=E_{x_n,t}+\gamma$, and the TM calculation tracks, from one plane to the next, the entire collection of locally optimal DPRM paths via the above prescription; the globally extremal path being the least energetic member of this ensemble of locally optimal paths [2]. All DP models possess similar rules, though $e3_{\mathrm{fcc}}$ and $g4_{\mathrm{bcc}}$ have no elastic energy cost built in, so $\gamma=0$.

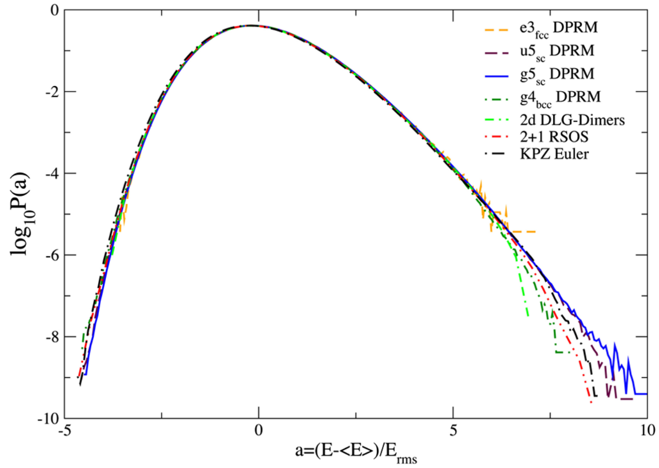


FIG. 1 (color online). Fluctuation PDFs: $2+1$ KPZ models.

For each $2+1$ DPRM model, we study initially the *full free-energy PDF* associated with the globally minimal trajectory documenting, as well, its rms fluctuation, skewness s, and kurtosis k. For the $u5_{\mathrm{sc}}$ DPRM, our gold standard, we simulated polymers of length $t=1000$, in an $L\times L$ system of transverse size $L=5000$, averaging over $nr=1880$ realizations of the random energy landscape, representing some 47 billion data points in our binned construction of the free energy PDF, shown in Fig. 1, a semilog plot. Similarly, $g5_{\mathrm{sc}}:(L,nr,t)=(10^4,432,10^3)$; $g4_{\mathrm{bcc}}:(L,nr,t)=(10^4,48,10^3)$; $e3_{\mathrm{fcc}}:(nr,t)=(10^7,500)$, all comply to a universal $2+1$ KPZ data collapse. Here, the abscissa $a\equiv(E-\langle E\rangle)/E_{\mathrm{rms}}$, the deviation scaled by the rms fluctuation, is the key dimensionless quantity. We also include in the figure our $2+1$ KPZ Euler integration, with $(L,nr,t)=(10^4,456,2000)$, a substantial numerical investment, quite beyond [18]; parameter values chosen were $(\lambda,\nu,D)=(20,\frac{1}{2},1)$, with white noise, and integration time step $\delta t=0.02$. We show too, in Fig 1, the height fluctuation PDFs of the $2+1$ RSOS and 2D driven dimer models; again $L=10^4$, with averaging over 136 and 12 runs, resp. For these two kinetic roughening models, as well as the KPZ equation itself, $a\equiv(h-\langle h\rangle)/h_{\mathrm{rms}}$, representing the *scaled height fluctuation*, as $h$ and $F$ are cognate variables in the stochastic growth and DPRM contexts. In any case, the severe data collapse for these 7 distinct members of the $2+1$ KPZ class provide us with strong evidence, indeed, of universality in this higher dimension, well into the tails.

To dig deep to the core of $2+1$ KPZ universality, and lay the groundwork for the remainder of this Letter, we now discuss in greater detail the full machinery of KPZ scaling theory, which rests upon a careful determination of the characteristic KPZ nonlinearity $\lambda$, as well as the static amplitude $A$, defined via the fixed-time height-height k-space correlator: $\langle |h(\mathbf{k})|^2 \rangle = Ak^{-2-2\chi}$. The essential ideas, laid out already for 1 + 1 KPZ [3], with additional helpful details from Kriecherbauer and Krug [5], focusses on the dimensionless time $\theta t$, where $\theta = A^{1/\chi}\lambda$, with $\chi$ the *steady-state* KPZ critical index. The basic KPZ narrative involves a bump on the surface of height $\xi_\perp$, lateral dimension $\xi_\parallel$, which evolves according to the KPZ nonlinear term as $\dot{\xi}_\parallel \approx \lambda(\xi_\perp/\xi_\parallel)$. With the transverse fluctuation scaling as $\xi_\perp \sim A\xi_\parallel^\chi$, consistency demands $\xi_\parallel \sim (A^2\lambda t)^{1/z}$ while $\xi_\perp \sim (\theta t)^{\beta=\chi/z}$, with $\theta$ as above, and dynamic index $z = 2 - \chi$ given by the KPZ identity. With the key scaling parameter $\theta$ known, universal KPZ amplitudes can be extracted for each model and compared across the 2 + 1 KPZ spectrum. Motivated by the exact 1 + 1 results of Sasamoto and Spohn [11], we conjecture that the solution of the 2 + 1 KPZ equation for 3D wedge (i.e., *conical*) IC centered at the origin has the form: $h(\mathbf{x}, t) = -x^2/2\lambda t + v_\infty t + (\theta t)^\beta \xi$ with the understanding that the statistics of the random variable $\xi$ has become the focus, and, *its PDF the definitive expression of* 2 + 1 *KPZ universality.* We have determined the KPZ early time exponent $\beta$ independently for each model; our DPRM, RSOS, and KPZ Euler results in fine accord with both revered [19], 0.240, and more recent [15] blue-chip estimates for this index. To pin down $P(\xi)$, and reveal its universal nature, we sift, anew, through the large data sets underlying the fluctuation PDFs of Fig. 1, recasting the analysis in terms of $\xi = (h - v_\infty t)/(\theta t)^\beta$, where, in the KPZ context, $v_\infty = \langle dh/dt \rangle$ is the asymptotic instantaneous growth velocity; analogously, $f_\infty = \langle dF/dt \rangle$, the DPRM free energy per unit length. It is the distribution $P(\xi)$ which lies at the heart of 2 + 1 KPZ class universality, and the matter demands, in addition to knowledge of $\theta$, a precise determination of KPZ-DPRM $v_\infty/f_\infty$. To this end, we have relied heavily upon a Krug-Meakin [20] finite-size scaling analysis which, by virtue of a truncated Fourier sum over modes, reveals that the KPZ growth velocity in a system of finite-size $L$ suffers a small shift from its true asymptotic value: $\Delta v \equiv \langle dh/dt \rangle - v_\infty = -\frac{1}{2}A\lambda/L^{2-2\chi}$; for the DPRM problem, the corresponding

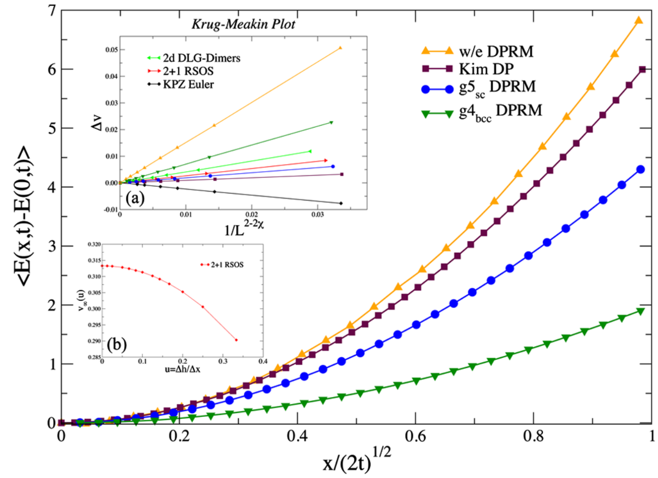


FIG. 2 (color online). Disorder-averaged, *parabolic* DPRM free energy profile. Insets: (a) Summary Krug-Meakin plot for 2 + 1 KPZ class models, (b) *quadratic* KPZ tilt-dependent growth velocity [23] for the 2 + 1 RSOS model.

*free energy shift* $\Delta f$ represents an ill-condensed matter manifestation of the Casimir effect [21]. In Fig. 2, we show results for our seven 2 + 1 KPZ class models—in fact, the first pass involves a 3-parameter fit, yielding $v_\infty$, the product $A\lambda$, and $\chi$; knowing $v_\infty$ and $\chi$, see Table I for values, allows construction of a summary Krug-Meakin plot of $\Delta v$ vs $1/L^{2-2\chi}$, including all 7 models, with slopes set by $-\frac{A\lambda}{2}$, see Fig 2(a). Via diverse procedures, it is also possible to extract the KPZ nonlinearity $\lambda$ directly; for the DPRM systems, we rely upon the *disorder-averaged quadratic free-energy profile,* an insight that dates back to Parisi and Mezard [22], but is implicit in our Sasamoto-Spohn conjecture above. Ultimately, it follows from the fact that at early times with conical IC, the KPZ nonlinearity dominates, generating Cole-Hopf paraboloids with small superposed distortions arising from the additive KPZ noise term. While such noise is visible for each individual run, ensemble averaging produces a smooth parabolic profile—see Fig 2, proper, which follows from $10^4$ realizations of our DPRM random energy landscape. Alternatively, for the KPZ stochastic growth models, such as 2 + 1 RSOS, we study the tilt-dependent growth velocity [23], Fig. 2(b). For 2D driven dimers, $A$ is known

TABLE I. 2 + 1 KPZ model parameters, *point-plane* DPRM geometry; equivalently, KPZ stochastic growth from a flat substrate.

| Model | $f_\infty(v_\infty)$ | $\lambda$ | $A$ | $\chi$ | $\theta$ | $\beta$ | $\langle\xi\rangle$ | $\langle\xi^2\rangle_c$ | $s$ | $k$ |
|---|---|---|---|---|---|---|---|---|---|---|
| $u5_{sc}$ Kim DP | 0.38390 | −0.1585 | 1.1978 | 0.389 | 0.2518 | 0.2402 | −0.714 | 0.250 | 0.422 | 0.343 |
| $g5_{sc}$ DPRM | −0.55336 | −0.2182 | 1.74215 | 0.381 | 0.9363 | 0.2425 | −0.675 | 0.211 | 0.433 | 0.356 |
| $e3_{fcc}$ DPRM | −2.64381 | −0.1439 | 21.03 | 0.387 | 375.3 | 0.248 | −0.754 | 0.208 | 0.435 | 0.362 |
| $g4_{bcc}$ DPRM | −1.80949 | −0.5014 | 2.8248 | 0.380 | 7.7198 | 0.235 | −0.851 | 0.240 | 0.412 | 0.320 |
| KPZ Euler | 0.17606 | 20 | 0.02295 | 0.388 | $1.192 \times 10^{-3}$ | 0.2408 | −0.690 | 0.243 | 0.418 | 0.343 |
| 2 + 1 RSOS | 0.31270 | −0.414 | 1.2005 | 0.383 | 0.66144 | 0.2422 | −0.737 | 0.233 | 0.427 | 0.349 |
| 2D DLG-dimers | 0.34141 | −0.6094 | 1.2201 | 0.375 | 1.0359 | 0.2415[a] | −0.830 | 0.256 | 0.414 | 0.338 |

[a]Ref. [15]

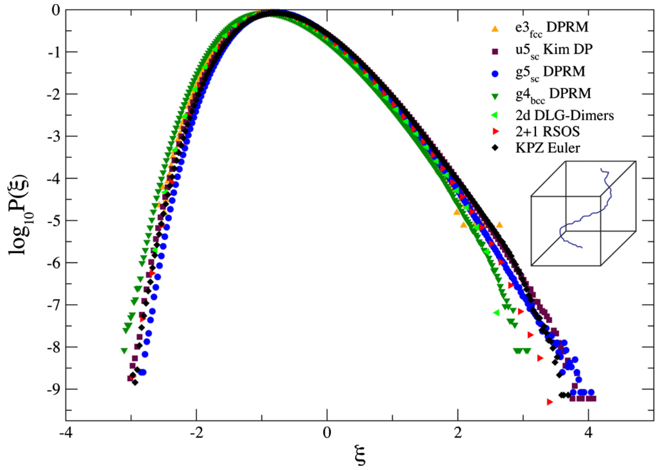


FIG. 3 (color online). Universal limit distribution, 2 + 1 KPZ class: DPRM *point-plane* geometry; KPZ stochastic growth with flat interface IC.

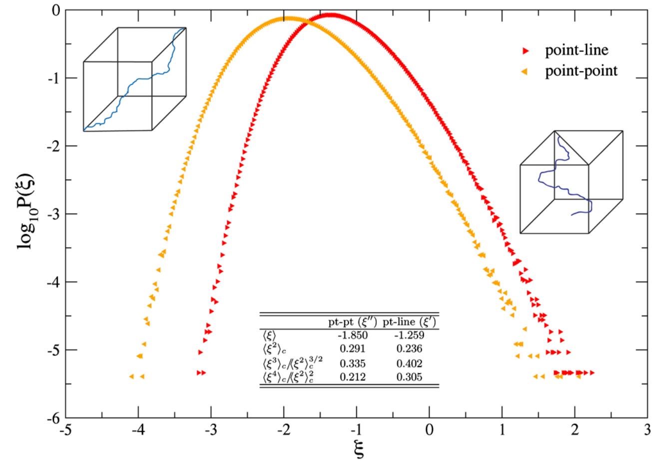


| | pt-pt ($\xi''$) | pt-line ($\xi'$) |
|---|---|---|
| $\langle\xi\rangle$ | -1.850 | -1.259 |
| $\langle\xi^2\rangle_c$ | 0.291 | 0.236 |
| $\langle\xi^3\rangle_c/\langle\xi^2\rangle_c^{3/2}$ | 0.335 | 0.402 |
| $\langle\xi^4\rangle_c/\langle\xi^2\rangle_c^2$ | 0.212 | 0.305 |

FIG. 4 (color online). Universal PDFs: 2 + 1 DPRM *point-point* and *point-line* geometries. Table inset: Distribution moments.

[15], so we get $\lambda$ directly from the Krug-Meakin plot. Recall all DPRM models, by default, have $\lambda < 0$; by contrast, our KPZ Euler integration was done with positive $\lambda = 20$. With $\theta$ and $f_\infty$ extracted for each of our models, refer to Table I, we can now craft a full portrait of 2 + 1 KPZ universality for the *point-plane* DPRM geometry, see Fig. 3; observe that, with respect to KPZ Euler, we have reversed the abscissa for our kinetic roughening and DPRM model results. In this much more stringent test of universality, we note several key points gleaned from Fig. 3 and associated Table I, where the final four columns record our model estimates for the mean, variance, skewness, and kurtosis of $P(\xi)$: (i) First, the existence of a unified 2 + 1 KPZ class, *per se,* is manifest. (ii) However, as in the case of 1 + 1 KPZ [24], there is a small, but persistent, dispersion among the models owing to a stubborn approach to asymptopia by the first moment $\langle\xi\rangle$; see, especially, $g4_{\mathrm{bcc}}$ DPRM. (iii) Skewness and kurtosis of the 2 + 1 KPZ *point-plane* problem are larger than TW GOE; an average over our KPZ models yields $\bar{s} = 0.424(7)$, $\bar{k} = 0.346(8)$, $\overline{\langle\xi^2\rangle_c} = 0.235(17)$, and $\overline{\langle\xi\rangle}/\sqrt{\langle\xi^2\rangle_c} = -1.45(9)$. Even so, the (iv) long right tail, as measured precisely by us for the $g5_{\mathrm{sc}}$ DPRM, has an exponent 1.495(10) nearly indistinguishable from the exact Airy value $\frac{3}{2}$, characteristic of the Tracy-Widom 1 + 1 KPZ class. We wonder whether, intuition to the contrary, the 2 + 1 KPZ case may possess some vestigial link to the Painlevé system and determinantal point processes, leaving open, perhaps, the possibility of a fulcrum, rational critical index.

Finally, in Fig. 4, we plot up the challenging distributions associated with the *point-line* and *point-point* geometries, studied by us with the wedge $e3_{\mathrm{fcc}}$ DPRM. In the 2 + 1 KPZ kinetic roughening context, these PDFs dictate height fluctuations for self-similar growth initiated, respectively, from point seed and 1D groove initial conditions, the former corresponding to TW GUE, the latter having no lower dimensional analog. We note here, particularly, that s and k increase in magnitude as one progresses from point-point, point-line, and point-plane problems, whereas the first and second moments trend in the opposite fashion, see Fig 4, table inset. We expect the point-point geometry, with extremal trajectories connecting far corners of the cube, will witness the first analytical advance; in its semidiscrete Poissonized DPRM form, it is germane to the generalized random permutation, plane partition, and polynuclear growth problems [9].

In summary, we have presented a complete, multifaceted portrait of 2 + 1 KPZ class universality, extracting the three characteristic PDFs associated with distinct DPRM point-plane, point-line, and point-point geometries. This represents a robust numerical solution of the 2 + 1 KPZ problem. It is our hope that this work will inspire experimentalists as well as anchor future analytical efforts, providing a target for physicists and mathematicians alike to shed light on the kinship of these limit distributions, and reveal its underlying superuniversal fixed point structure. Given the replica-theoretic interpretation of the 2 + 1 DPRM, explicit calculation of any one of our numerical PDFs would not only reveal much regarding KPZ stochastic growth phenomena and DLG interacting particle systems, but also the foundational statistical mechanical problem of attractive bosons in two dimensions.

We are grateful to J. Krug and E. Brézin for illuminating, very helpful discussions regarding our work. This research was supported, in part, by NSF Grant No. DMR-0434500 and a well-timed Spring 2012 Barnard College SFRL.

[1] M. Kardar, G. Parisi, and Y.-C. Zhang, Phys. Rev. Lett. **56**, 889 (1986).
[2] T. Halpin-Healy and Y.-C. Zhang, Phys. Rep. **254**, 215 (1995); J. Krug, Adv. Phys. **46**, 139 (1997).

[3] J. Krug, P. Meakin, and T. Halpin-Healy, Phys. Rev. A **45**, 638 (1992); J. Amar and F. Family, Phys. Rev. A **45**, 5378 (1992).

[4] J. M. Kim, M. A. Moore, and A. J. Bray, Phys. Rev. A **44**, 2345 (1991); T. Halpin-Healy, Phys. Rev. A **44**, R3415 (1991).

[5] T. Kriecherbauer and J. Krug, J. Phys. A **43**, 403001 (2010); I. Corwin, arXiv:1106.1596; A. Borodin and I. Corwin, arXiv:1111.4408.

[6] K. Johansson, Commun. Math. Phys. **209**, 437 (2000).

[7] P. Meakin, P. Ramanlal, L. M. Sander, and R. C. Ball, Phys. Rev. A **34**, 5091 (1986).

[8] C. Tracy and H. Widom, Commun. Math. Phys. **159**, 151 (1994); C. Tracy and H. Widom, *ibid.* **177**, 727 (1996); C. Tracy and H. Widom, *ibid.* **207**, 665 (1999).

[9] M. Prähofer and H. Spohn, Phys. Rev. Lett. **84**, 4882 (2000); A. Okounkov, arXiv:math/0309074.

[10] J. Baik, P. Deift, and K. Johansson, J. Am. Math. Soc. **12**, 1119 (1999).

[11] T. Sasamoto and H. Spohn, Phys. Rev. Lett. **104**, 230602 (2010); G. Amir, I. Corwin, and J. Quastel, Commun. Pure Appl. Math. **64**, 466 (2011).

[12] P. Calabrese, P. Le Doussal, and A. Rosso, Europhys. Lett. **90**, 20002 (2010); V. Dotsenko, *ibid.* **90**, 20003 (2010); for $1 + 1$ GOE, rather than GUE, DPRM see P. Calabrese and P. Le Doussal, Phys. Rev. Lett. **106**, 250603 (2011).

[13] K. A. Takeuchi and M. Sano, Phys. Rev. Lett. **104**, 230601 (2010); also, K. A. Takeuchi, M. Sano, T. Sasamoto, and H. Spohn, Sci. Rep. (Nature) **1**, 34 (2011).

[14] H. Spohn, arXiv:1201.0645.

[15] J. Kelling and G. Ódor, Phys. Rev. E **84**, 061150 (2011); G. Ódor, B. Liedke, and K.H. Heinig, Phys. Rev. E **79**, 021125 (2009).

[16] J. Krug and T. Halpin-Healy, J. Phys. A **31**, 5939 (1998).

[17] J. Olejarz, P. L. Krapivsky, S. Redner, and K. Mallick, Phys. Rev. Lett. **108**, 016102 (2012).

[18] K. Moser, J. Kertész, and D. E. Wolf, Physica (Amsterdam) **A178**, 215 (1991).

[19] B. M. Forrest and L.-H. Tang, Phys. Rev. Lett. **64**, 1405 (1990).

[20] J. Krug and P. Meakin, J. Phys. A **23**, L987 (1990).

[21] J. Krug and L.-H. Tang, Phys. Rev. E **50**, 104 (1994).

[22] G. Parisi, J. Phys. (Paris) **51**, 1595 (1990); M. Mézard, *ibid.* **51**, 1831 (1990).

[23] J. Krug and H. Spohn, Phys. Rev. Lett. **64**, 2332 (1990).

[24] P. Ferrari and R. Frings, J. Stat. Phys. **144**, 1123 (2011).